Cell

Operational Plasticity Enables Hsp104 to Disaggregate Diverse Amyloid and Nonamyloid Clients

Morgan E. DeSantis,[1,2] Eunice H. Leung,[1] Elizabeth A. Sweeny,[1,2] Meredith E. Jackrel,[1] Mimi Cushman-Nick,[1,3] Alexandra Neuhaus-Follini,[1,3] Shilpa Vashist,[1] Matthew A. Sochor,[1,2] M. Noelle Knight,[1,2] and James Shorter[1,2,3,*]
[1]Department of Biochemistry and Biophysics
[2]Biochemistry and Molecular Biophysics Graduate Group
[3]Neuroscience Graduate Group
Perelman School of Medicine, University of Pennsylvania, Philadelphia, PA 19104, USA
*Correspondence: jshorter@mail.med.upenn.edu
http://dx.doi.org/10.1016/j.cell.2012.09.038

SUMMARY

It is not understood how Hsp104, a hexameric AAA+ ATPase from yeast, disaggregates diverse structures, including stress-induced aggregates, prions, and α-synuclein conformers connected to Parkinson disease. Here, we establish that Hsp104 hexamers adapt different mechanisms of intersubunit collaboration to disaggregate stress-induced aggregates versus amyloid. To resolve disordered aggregates, Hsp104 subunits collaborate noncooperatively via probabilistic substrate binding and ATP hydrolysis. To disaggregate amyloid, several subunits cooperatively engage substrate and hydrolyze ATP. Importantly, Hsp104 variants with impaired intersubunit communication dissolve disordered aggregates, but not amyloid. Unexpectedly, prokaryotic ClpB subunits collaborate differently than Hsp104 and couple probabilistic substrate binding to cooperative ATP hydrolysis, which enhances disordered aggregate dissolution but sensitizes ClpB to inhibition and diminishes amyloid disaggregation. Finally, we establish that Hsp104 hexamers deploy more subunits to disaggregate Sup35 prion strains with more stable "cross-β" cores. Thus, operational plasticity enables Hsp104 to robustly dissolve amyloid and nonamyloid clients, which impose distinct mechanical demands.

INTRODUCTION

Several fatal neurodegenerative disorders, including Parkinson disease (PD), are connected with the misfolding of specific proteins into soluble toxic oligomers and stable cross-β fibers, termed amyloid (Cushman et al., 2010). Amyloidogenesis is also a severe problem in recombinant protein purification from diverse systems ranging from bacteria to animal cells. Here, overexpressed proteins form inclusions and adopt the amyloid form (Wang et al., 2008). Thus, amyloid frustrates basic structural and functional studies and limits production of valuable therapeutic proteins in the pharmaceutical sector. The dearth of solutions to these problems reflects a profound gap in our understanding of how cells safely reverse amyloid formation.

Amyloid disaggregation is coupled to degradation in animal cell extracts, but the identity of the disaggregase is unknown (Cohen et al., 2006). Moreover, Hsp110, Hsp70, and Hsp40, the metazoan protein-disaggregase system, cannot rapidly disaggregate amyloid (Shorter, 2011). Perplexingly, animals lack Hsp104 orthologs, which are found in bacteria, fungi, protozoa, chromista, and plants. Hsp104 is a hexameric, ring-shaped translocase with two AAA+ nucleotide-binding domains (NBDs) per subunit that couple ATP hydrolysis to protein disaggregation (Vashist et al., 2010). In yeast, Hsp104 promotes survival of protein-folding stress by collaborating with Hsp70 and Hsp40 to renature the entire aggregated proteome (Parsell et al., 1994; Vashist et al., 2010). Thioflavin-T (ThT) fluorescence, Congo red binding, sedimentation, electron microscopy, and SDS resistance have been used to establish that Hsp104 rapidly remodels various amyloid forms, including Sup35 and Ure2 prions. Hsp104 also rapidly eliminates preamyloid oligomers that accumulate prior to fibers (Shorter and Lindquist, 2004, 2006). Thus, Hsp104 enables yeast to harness infectious amyloids, termed prions, for beneficial purposes (Halfmann et al., 2012; but see also Wickner et al., 2011). How Hsp104 disaggregates such a diverse repertoire of structures, ranging from stable amyloid to less stable disordered aggregates (Knowles et al., 2007; Wang et al., 2010), is not understood. This immense substrate diversity imposes extreme mechanical demands on Hsp104.

The loss of Hsp104 from metazoa is baffling. Transgenic mice expressing Hsp104 are normal, and Hsp104 increases stress tolerance of animal cells (Dandoy-Dron et al., 2006). Moreover, Hsp104 directly remodels PD-associated oligomers and amyloids formed by α-synuclein (α-syn) and rescues rodent models of PD and Huntington disease (HD) (Lo Bianco et al., 2008; Vacher et al., 2005). Thus, Hsp104 could be developed as a therapeutic disaggregase for neurodegenerative disorders (Vashist et al., 2010).

Ideally, to optimize therapy and minimize side effects, Hsp104 would be engineered and potentiated to dissolve specific aggregates central to the disease in question (Vashist et al., 2010). Indeed, Hsp104's disaggregase activity could be enhanced and tailored for any protein. Thus, substrate-optimized Hsp104 variants could increase protein solubility and enable facile purification of recalcitrant proteins in diverse settings. However, limited structural and mechanistic understanding of Hsp104 hexamers frustrates such endeavors. It is not understood how individual subunits of the Hsp104 hexamer coordinate substrate translocation and ATP hydrolysis to solubilize unrelated proteins trapped in energetically and structurally distinct aggregates (Doyle et al., 2007b; Lee et al., 2010; Tessarz et al., 2008; Wendler et al., 2007, 2009).

Do Hsp104 hexamers use the same mechanism to disaggregate amyloid and nonamyloid clients? Specific mutations in Hsp104 differentially affect its activity against prions and disordered aggregates, as does ATPγS, a slowly hydrolyzable ATP analog, suggesting a mechanistic dichotomy or plasticity (Doyle et al., 2007b; Kurahashi and Nakamura, 2007). This dichotomy might reflect an ability of Hsp104 subunits to collaborate differently to promote dissolution of diverse aggregated structures.

How individual subunits collaborate to promote substrate remodeling is a key question not only for Hsp104 but for all NTP-fueled, hexameric ring-translocases. Several different intersubunit collaboration models have been proposed, including (1) probabilistic models in which individual subunits function noncooperatively and independently (Martin et al., 2005); (2) models of subglobal cooperativity where a subset of subunits cooperate (Moreau et al., 2007); and (3) models of global cooperativity in which all subunits cooperate in sequence or in concert (Lyubimov et al., 2011). Typically, these models focus on coordination of NTPase events. Less attention has been given to how individual subunits within the hexamer contribute to substrate binding and translocation. For example, it is not clear whether globally cooperative ATPase activity must invariably be coupled to globally cooperative substrate handling. A key unresolved issue is whether a single ring-translocase can exploit different modes of intersubunit collaboration to remodel substrates that impose disparate mechanical demands.

Here, we elucidate that Hsp104 subunits collaborate via radically different mechanisms to disaggregate disordered aggregates versus amyloid. Unexpectedly, the *E. coli* homolog of Hsp104, ClpB, coordinates subunit collaboration differently than Hsp104, even though Hsp104 and ClpB are widely assumed to function by the same mechanism (Doyle and Wickner, 2009). Hsp104 exhibits operational plasticity that confers adaptable disaggregase activity suited for the demands of the yeast proteome, which include prion disaggregation. In contrast, ClpB is finely tuned for optimal disordered aggregate dissolution and has limited ability to dissolve amyloid.

RESULTS

Experimental Logic

We employed a mutant doping strategy to determine the contribution of individual subunits toward protein disaggregation and thereby define mechanochemical coupling mechanisms of Hsp104 hexamers. Thus, mutant subunits defective in ATP hydrolysis or substrate binding are mixed with wild-type (WT) subunits to generate heterohexamer ensembles according to a binomial distribution that is determined by the WT:mutant ratio (Figure 1A). This strategy has yielded key insights for other NTP-fueled ring-translocases but is dependent upon random mixing of mutant and WT subunits at the monomer level (Moreau et al., 2007; Werbeck et al., 2008).

First, we employed several techniques to verify statistical WT and mutant Hsp104 (Hsp104^{DPL}, Hsp104^{DWA}, Hsp104^{DWB}, or Hsp104^{DWBDPL}) subunit mixing and heterohexamer ensemble formation. These techniques included (1) affinity chromatography to separate heterohexamers with different numbers of biotinylated subunits (Figures S1A–S1D available online) or different numbers of his-tagged subunits (Figures S1E–S1I); (2) kinetic sensitivity of Hsp104-catalyzed green fluorescent protein (GFP) disaggregation to excess mutant subunit (Figure S1J); and (3) fluorescence energy transfer between labeled subunits to detect subunit mixing within Hsp104 hexamers (Figures S2A–S2J). Thus, we establish that (1) Hsp104 forms dynamic hexamers that rapidly exchange subunits on the minute timescale (Figures S1A–S1J and S2A–S2J) similar to ClpB (Werbeck et al., 2008) and (2) specific mutant subunits (Hsp104^{DPL}, Hsp104^{DWA}, Hsp104^{DWB}, or Hsp104^{DWBDPL}) defective in substrate binding or ATP hydrolysis (or both) incorporate statistically into WT hexamers just as well as WT subunits (Figures S1A–S1J and S2A–S2J). Thus, Hsp104 provides a highly tractable system for mutant doping studies.

Importantly, this rapid and statistical subunit exchange allows generation of heterohexamer ensembles comprised of WT and mutant subunits according to a binomial distribution that varies as a function of the molar ratio of each subunit (Figures 1A and S1D–S1I; see Extended Experimental Procedures) (Werbeck et al., 2008). Using this distribution, we can predict how disaggregase activity would be inhibited at various mutant:WT ratios if a specified number of mutant subunits inactivate the hexamer (Figure 1B; see Extended Experimental Procedures). Thus, if all six subunits must work together, then one mutant subunit would abolish hexamer activity (Figure 1B, dark blue curve). If the activity of a single subunit within the hexamer is sufficient, then some activity would still be observed with five mutant subunits per hexamer, and only six mutant subunits would abolish activity (Figure 1B, orange line). By comparing experimental data with theoretical plots, we can determine whether subunit collaboration within Hsp104 hexamers is probabilistic (six mutant subunits abolish activity), subglobally cooperative (two to five mutant subunits abolish activity), or globally cooperative (one mutant subunit abolishes activity).

Hsp104 Uses a Probabilistic Mechanism to Dissolve Disordered Aggregates

To define how Hsp104 subunits coordinate substrate binding, we employed Hsp104^{DPL}, which harbors Y257A and Y662A mutations in the NBD1 and NBD2 channel loops that impair substrate binding (Lum et al., 2008). Importantly, Hsp104^{DPL} has WT ATPase activity (Figure 1C), incorporates into WT

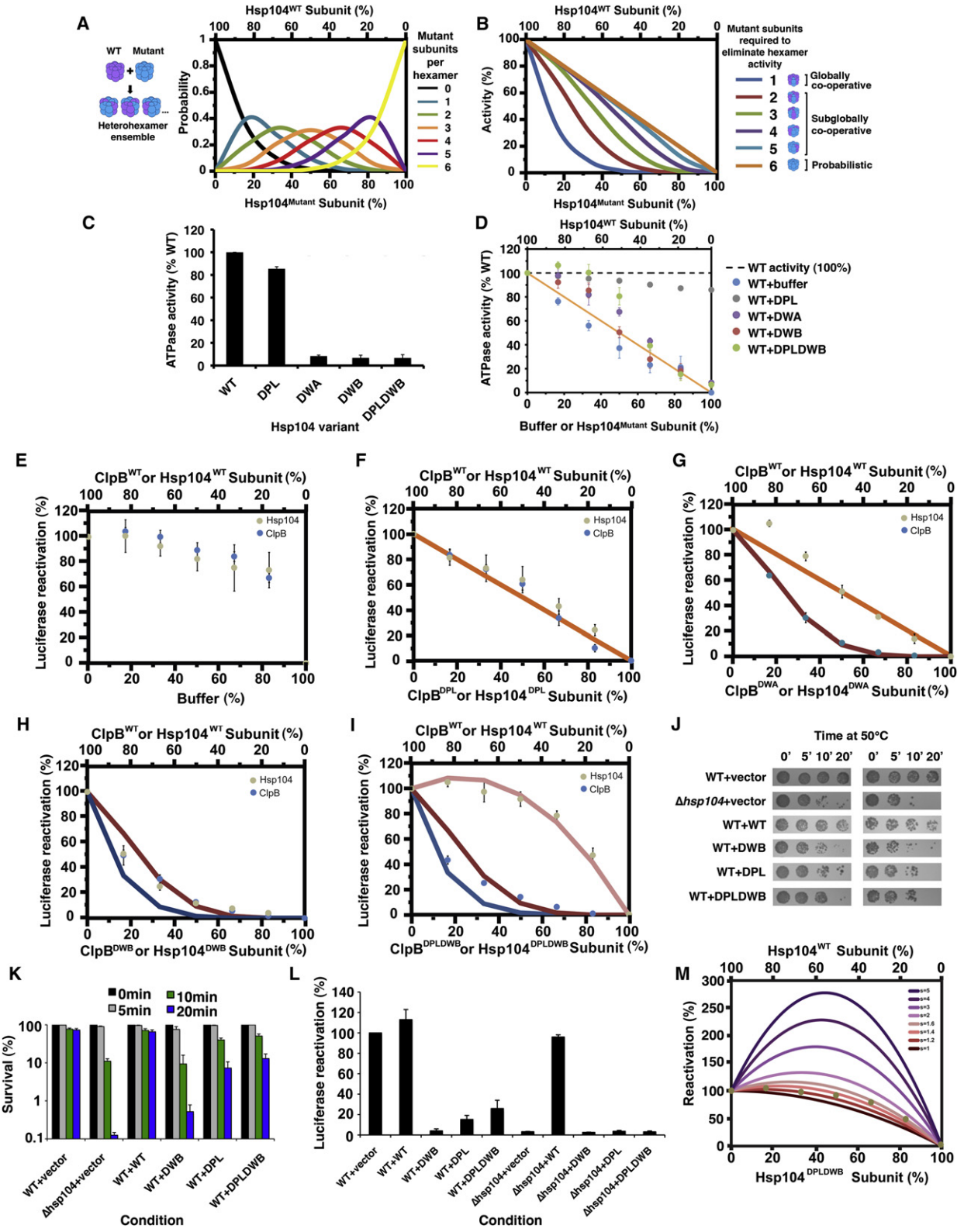

Figure 1. Hsp104 Uses a Probabilistic Mechanism to Dissolve Disordered Aggregates

(A) Theoretical Hsp104 hexamer ensembles containing zero (black), one (blue), two (green), three (orange), four (red), five (purple), and six mutant subunits (yellow) as a function of the fraction of mutant subunit present.

hexamers just as well as WT Hsp104 (Figures S1D–S1F and S2J), and has minimal effect on total ATPase activity when mixed with WT Hsp104 (Figure 1D, gray markers).

We assembled heterohexamer ensembles of WT Hsp104 and Hsp104^{DPL} and assessed disaggregase activity against disordered luciferase aggregates. Dilution of Hsp104 with buffer had little effect, whereas addition of Hsp104^{DPL} caused a roughly linear decline in disaggregase activity (Figures 1E and 1F). Similar data were obtained with heat-denatured GFP aggregates and heat-denatured citrate synthase (CS) aggregates (Figures S3A and S3B). This tolerance of Hsp104 hexamers to Hsp104^{DPL} subunits suggests that, for disordered aggregates, Hsp104 translocates substrate in a probabilistic manner. Thus, a single WT subunit per hexamer can catalyze disaggregation.

This probabilistic mechanism of substrate handling is conserved over 2 billion years of evolution to *E. coli* ClpB. ClpB displayed a roughly linear decline in luciferase disaggregation activity in response to a substrate-binding-defective variant, ClpB^{DPL} (Y251A:Y653A) (Weibezahn et al., 2004), whereas buffer had no effect (Figures 1E and 1F).

This noncooperative substrate handling was surprising because Hsp104 cooperatively hydrolyzes ATP (Hattendorf and Lindquist, 2002). To determine the role of individual subunits with respect to ATP hydrolysis, we utilized ATPase-defective Hsp104^{DWA}, which harbors K218T and K620T mutations in the NBD1 and NBD2 Walker A motifs. These mutations severely inhibit ATP hydrolysis (Figure 1C) by reducing affinity for ATP but do not impair hexamerization at the Hsp104 concentrations employed here (Schirmer et al., 2001). Indeed, Hsp104^{DWA} incorporated into WT hexamers just like WT Hsp104 (Figures S1C–S1E, S1G, and S2J). Doping revealed that Hsp104^{DWA} subunits inhibited total ATPase activity slightly less than predicted by a linear response (Figure 1D, compare purple markers to orange line). Strikingly, Hsp104^{DWA} subunits elicited a roughly linear decline in luciferase, GFP, and CS disaggregation by Hsp104 (Figures 1G, S3C, and S3D). Thus, Hsp104 couples probabilistic ATPase activity and substrate handling to disordered aggregate dissolution, indicating that the Hsp104 power stroke can be generated by ATP hydrolysis in a single subunit.

ClpB Hexamers Are Tuned Differently to Hsp104 Hexamers

These findings were surprising because mutant doping with ClpB indicated that highly cooperative ATP hydrolysis powers disordered aggregate dissolution (Hoskins et al., 2009). Indeed, ATPase-defective ClpB^{DWA} (K212T:K611T) caused a sharp nonlinear decline in ClpB disaggregase activity, which is consistent with two mutant subunits abolishing hexamer activity (Figures 1B and 1G). We also assessed ClpB^{DWB}, which bears E279Q and E678Q mutations in the NBD1 and NBD2 Walker B motifs. ClpB^{DWB} forms hexamers that bind but do not hydrolyze ATP (Weibezahn et al., 2003). Doping ClpB^{DWB} elicited a sharp nonlinear decline in disaggregase activity such that one to two mutant subunits abolish hexamer activity (Figures 1B and 1H). Thus, unlike Hsp104, ClpB subunits couple highly collaborative ATPase activity to probabilistic substrate handling to dissolve disordered aggregates.

ClpB^{DWB} is a substrate "trap" (Weibezahn et al., 2003), which might poison WT hexamers by not releasing substrate rather than by perturbing intersubunit coordination of ATP hydrolysis. To address this issue, we constructed ClpB^{DPLDWB} in which the substrate-binding pore loops and Walker B motifs are mutated (Y251A:E279Q:Y653A:E678Q). Doping ClpB^{DPLDWB} caused a sharp decline in luciferase reactivation such that one to two mutant subunits ablated activity (Figure 1I). Thus, substrate binding by ClpB^{DWB} does not poison WT hexamers. Rather, five to six ClpB subunits per hexamer must hydrolyze ATP for protein disaggregation. Surprisingly, this highly coordinated ATPase pattern of ClpB hexamers is coupled to stochastic substrate binding (Figures 1F–1H).

Hsp104 Hexamers Tolerate Multiple Subunits Defective in ATP Hydrolysis and Substrate Binding

We obtained dissimilar results with Hsp104. Hsp104^{DWB} (E285Q:E687Q) and Hsp104^{DPLDWB} (Y257A:E285Q:Y662A:E687Q) have little ATPase activity and incorporate into WT hexamers as predicted (Figures 1C, S1D, S1E, S1H, S1I, S2J). Like Hsp104^{DWA}, Hsp104^{DWB} subunits caused a roughly linear decline in total ATPase activity (Figure 1D, compare red markers to orange

(B) Theoretical activity curves where one or more (blue), two or more (red), three or more (green), four or more (purple), five or more (light blue), or six mutant subunits (orange) are needed to ablate hexamer activity.

(C) WT or mutant Hsp104 ATPase activity. Values represent means ±SEM (n = 3–5).

(D) Hsp104 was mixed with increasing fractions of mutant Hsp104 proteins or buffer, and ATPase activity was assessed. Values represent means ±SEM (n = 3–5). Orange line indicates expected ATPase activity if six mutant subunits are needed to ablate hexamer activity.

(E–I) Luciferase aggregates were treated with Hsp104 (gray markers), Hsc70 (an Hsp70), and Hdj2 (an Hsp40) plus increasing fractions of buffer (E), Hsp104^{DPL} (F), Hsp104^{DWA} (G), Hsp104^{DWB} (H), or Hsp104^{DPLDWB} (I). Alternatively, luciferase aggregates were treated with ClpB (blue markers), DnaK, DnaJ, and GrpE plus increasing fractions of buffer (E), ClpB^{DPL} (F), ClpB^{DWA} (G), ClpB^{DWB} (H), or ClpB^{DPLDWB} (I). Luciferase reactivation (% WT activity) was then assessed. Values represent means ±SEM (n = 3–4). Theoretical disaggregase activity if six (orange line [F and G]), two or more (red line [G–I]), or one or more mutant subunits (blue line [H and I]) ablate hexamer activity. Pink line (I) indicates simulated activity if a mutant subunit stimulates an adjacent WT subunit 1.4-fold but is inhibitory if adjacent to a mutant subunit.

(J and K) WT yeast carrying the indicated Hsp104 plasmid or Δ*hsp104* yeast harboring an emptor vector control were treated at 50°C for 0–20 min and then spotted (J). The spotting on the right is a 5-fold dilution of the spotting on the left. Alternatively, cells were plated and survival (%) was calculated (K). Values represent means ±SEM (n = 3).

(L) WT or Δ*hsp104* yeast expressing luciferase and the indicated Hsp104 variant were shifted to 44°C, treated with cycloheximide, and allowed to recover at 30°C. Luciferase activity (% of the WT+vector control) was determined. Values represent means ±SEM (n = 3).

(M) Adjacent pairs of WT-WT or WT mutant subunits determine hexamer activity, whereas adjacent mutant subunits have no activity. Each adjacent WT-WT pair has an activity of 1/6. By contrast, adjacent WT mutant pairs have a stimulated activity (s), and the effect of various values of s is depicted. Brown markers indicate experimental luciferase disaggregation data obtained with Hsp104^{DPLDWB}.

See also Figures S1, S2, and S3.

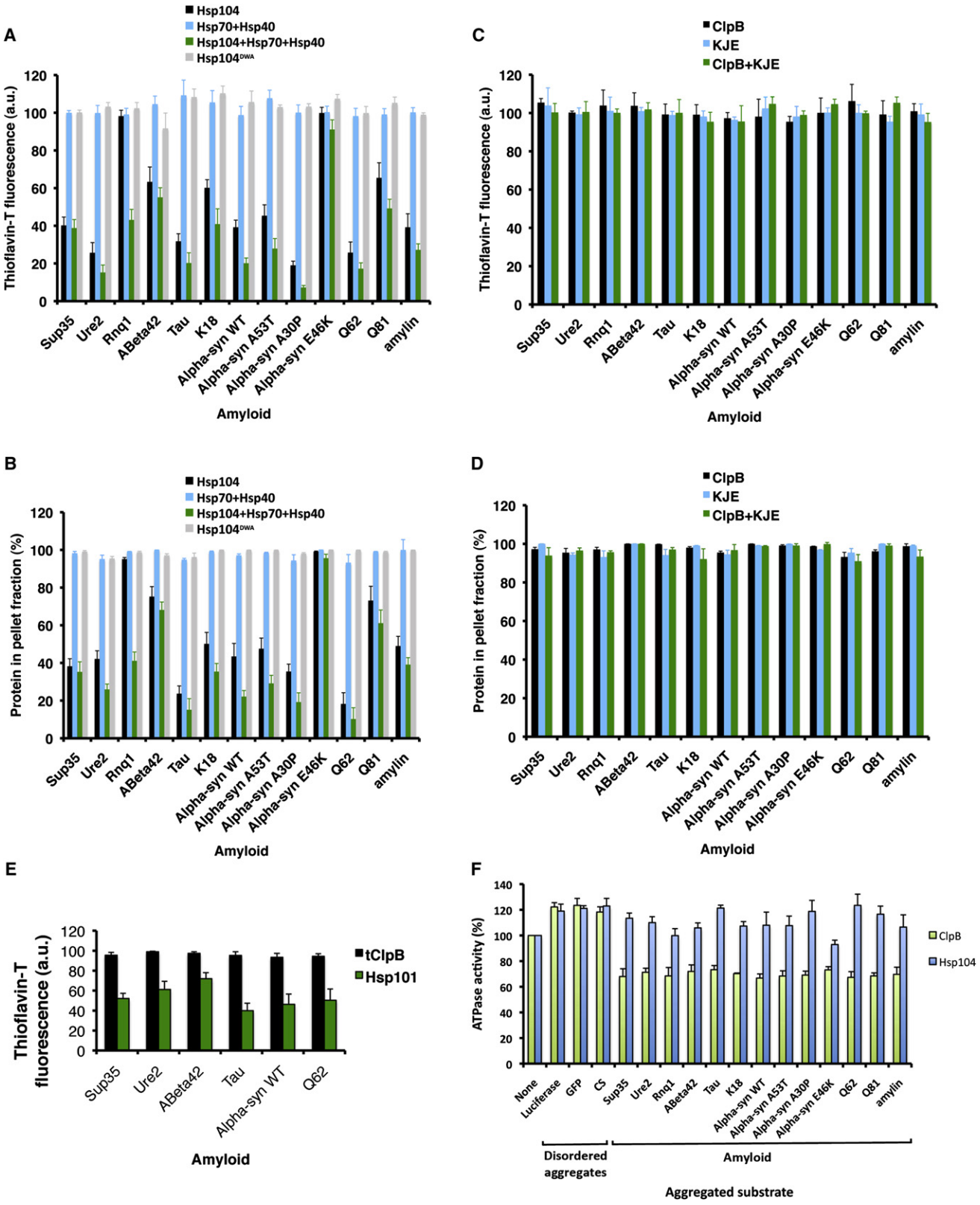
A
Hsp104
Hsp70+Hsp40
Hsp104+Hsp70+Hsp40
Hsp104DWA
Thioflavin-T fluorescence (a.u.)
120
100
80
60
40
20
0
Sup35
Ure2
Rnq1
ABeta42
Tau
K18
Alpha-syn WT
Alpha-syn A53T
Alpha-syn A30P
Alpha-syn E46K
Q62
Q81
amylin
Amyloid
C
ClpB
KJE
ClpB+KJE
Thioflavin-T fluorescence (a.u.)
Amyloid
B
Protein in pellet fraction (%)
Amyloid
D
Protein in pellet fraction (%)
Amyloid
E
Thioflavin-T fluorescence (a.u.)
tClpB
Hsp101
Amyloid
F
ATPase activity (%)
140
120
100
80
60
40
20
0
ClpB
Hsp104
None
Luciferase
GFP
CS
Disordered aggregates
Amyloid
Aggregated substrate

line). In contrast, Hsp104^{DPLDWB} had little effect on total ATPase activity unless the fraction of mutant subunit exceeded 50%, in which case inhibition was similar to Hsp104^{DWB} (Figure 1D, compare green to red markers). Similar to ClpB, one to two Hsp104^{DWB} subunits per hexamer abolished disaggregase activity (Figures 1H, S3E, and S3F). Unlike ClpB, inhibition was partially rescued by the substrate-binding loop mutations in Hsp104^{DPLDWB} (Figures 1I, S3G, and S3H). Thus, it is not the ATPase defect but "substrate trapping" by a single Hsp104^{DWB} subunit that poisons a hexamer with five WT subunits. Indeed, Hsp104^{DWA} confers a similar ATPase defect to Hsp104^{DWB} (Figure 1D) but cannot interact with substrate (Bösl et al., 2005) and does not elicit a sharp decline in disaggregase activity (Figures 1G and 1H). Consistent with these in vitro findings, Hsp104^{DWB} has a more severe dominant-negative effect than Hsp104^{DPL} or Hsp104^{DPLDWB} on Hsp104 function in thermotolerance and luciferase disaggregation in vivo (Figures 1J–1L).

The response to Hsp104^{DPLDWB} subunits was unusual. Rather than a linear decline, we observed little effect at low fractions of Hsp104^{DPLDWB} and a sharp decline when the fraction of Hsp104^{DPLDWB} subunit exceeded 66.7% (Figure 1I). We could model this behavior if we imposed rules whereby a mutant subunit stimulates the activity of an adjacent WT subunit by ~1.4-fold but exerts an inhibitory effect if it is adjacent to a mutant subunit (Figures 1I, S3G, and S3H, compare pink line to gray markers; see Extended Experimental Procedures and Figure 1M). Thus, Hsp104 hexamers operate via principles distinct from those of ClpB hexamers. The Hsp104 hexamer displays greater plasticity. It tolerates a wider variety of subunit-inactivating events without gross perturbations in disaggregase activity. For example, an Hsp104 subunit that (1) binds but cannot hydrolyze ATP and (2) is unable to engage substrate can stimulate the disaggregase activity of an adjacent subunit. In ClpB, a single subunit with these properties inactivates the entire hexamer.

Hsp104 Remodels Diverse Amyloids, Whereas ClpB Has Limited Activity

Hsp104 plasticity might ensure inheritance of numerous beneficial prions (Alberti et al., 2009). By contrast, although *E. coli* exploits functional amyloid on the cell surface, it is not known to harbor cytoplasmic prions and barely supports Sup35 prion formation (Barnhart and Chapman, 2006; Garrity et al., 2010). Indeed, ClpB has limited ability to remodel Sup35 prions (Reidy et al., 2012; Shorter and Lindquist, 2004). However, it is unknown whether this limitation extends to other amyloids.

We tested whether Hsp104 and ClpB disaggregated various amyloids formed by proteins with diverse primary sequences, including yeast prion proteins Sup35, Ure2, and Rnq1. We also tested whether Hsp104 and ClpB disaggregated various amyloids formed by proteins linked to Alzheimer disease, PD, HD, or type 2 diabetes, such as Aβ42, tau (and K18, a tau fragment), α-syn (WT and PD-linked variants: A53T, A30P, and E46K), polyglutamine (Q62 and Q81), and amylin (Cushman et al., 2010). Hsp104^{DWA} was inactive, but Hsp104 remodeled the majority of these amyloids in a manner that was slightly enhanced by Hsp70 (Ssa1) and Hsp40 (Sis1), which were inactive alone (Figures 2A and 2B). Rnq1 prions were an exception that necessitated Hsp70 and Hsp40, whereas α-syn^{E46K}, Aβ42, and Q81 amyloids were generally more refractory (Figures 2A and 2B). Thus, Hsp70 and Hsp40 are not always essential for Hsp104 to disaggregate diverse cross-β structures. We suggest that a generic feature of amyloid unleashes Hsp104 disaggregase activity in the absence of Hsp70 and Hsp40.

ClpB had limited ability to disaggregate amyloid with or without Hsp70 (DnaK) and Hsp40 (DnaJ) (Figures 2C and 2D). Indeed, we varied ClpB, DnaK, DnaJ, and GrpE concentration (0–50 μM), incubation time (0–96 hr), and ATP concentration (0–25 mM) but could not establish conditions in which ClpB disaggregated amyloid. Similarly, ClpB from *T. thermophilus* was unable to disaggregate amyloid, whereas the *A. thaliana* homolog, Hsp101, remodeled various amyloids (Figure 2E).

The low ClpB activity might reflect a lack of unknown cofactors that enable amyloid disaggregation. However, *E. coli* cytosol had limited ability to disaggregate amyloid and did not stimulate ClpB (Figure S4A). In contrast, yeast cytosol remodeled diverse amyloids, whereas Δ*hsp104* yeast cytosol did not unless supplemented with Hsp104 (Figure S4B). Thus, the failure of *E. coli* cytosol to stimulate amyloid disaggregation by ClpB indicated that cofactors were not missing and that ClpB has limited amyloid-disaggregase activity.

The inability of ClpB to disaggregate amyloid (Figures 2C and 2D) might reflect a reduced binding affinity for amyloid. Yet, the K_d of ClpB and Hsp104 for each amyloid and disordered aggregate used here was similar and ranged from ~30–100 nM (Table S1). Thus, some aspect of amyloid antagonizes ClpB, but not Hsp104, after initial engagement.

ClpB is more sensitive than Hsp104 to ATPase-defective subunits (Figures 1G and 1I). Thus, amyloid might inhibit the ATPase activity of sufficient ClpB subunits per hexamer to ablate activity. Indeed, amyloids inhibited ClpB ATPase activity by ~30%, whereas disordered aggregates stimulated by ~20% (Figure 2F). Hsp104 ATPase activity was stimulated by disordered aggregates and several amyloids, but some amyloids had no effect (Figure 2F). Thus, amyloid specifically inhibits ClpB ATPase activity, which might explain ClpB's limited amyloid-disaggregase activity.

Figure 2. Hsp104 Disaggregates Diverse Amyloids, Whereas ClpB Does Not

(A–D) Sup35, Ure2, Rnq1 or Aβ42, tau, K18, α-syn^{WT}, α-syn^{A53T}, α-syn^{A30P}, α-syn^{E46K}, Q62, Q81, and amylin amyloids were treated with the indicated combination of Hsp104, Ssa1, Sis1, or Hsp104^{DWA} (A and B) or ClpB, DnaK, DnaJ, and GrpE (C and D). Fiber integrity was assessed by ThT fluorescence (A and C) or sedimentation (B and D). Values represent means ±SEM (n = 3).

(E) Sup35, Ure2, Aβ42, tau, α-syn^{WT}, and Q62 amyloids were treated with tClpB or Hsp101. Fiber integrity was assessed by ThT fluorescence. Values represent means ±SEM (n = 3).

(F) ATPase activity of ClpB or Hsp104 in the presence of the indicated aggregated substrate. Values represent means ±SEM (n = 3).

See also Figure S4 and Table S1.

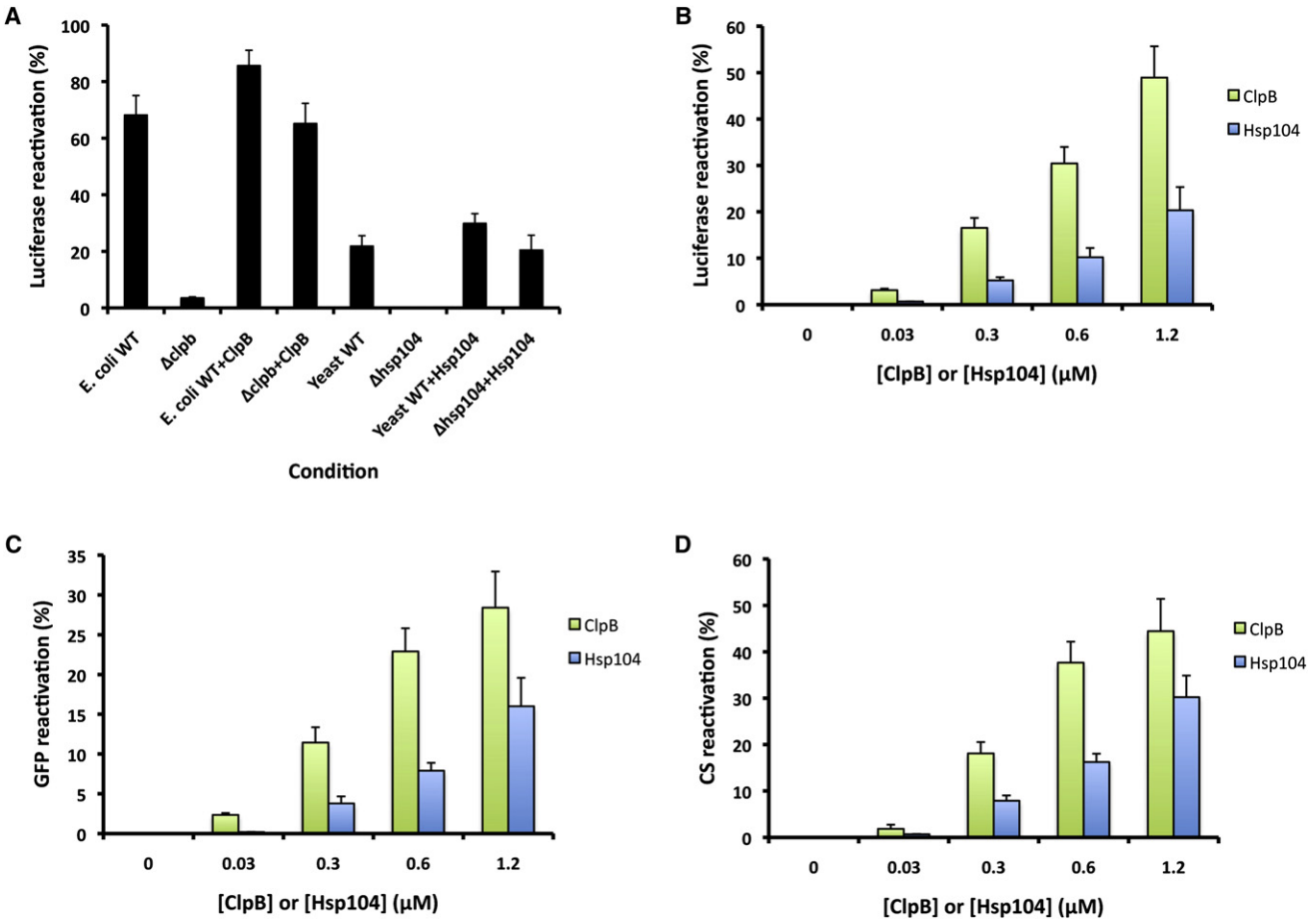

Figure 3. ClpB Reactivates Disordered Aggregates More Effectively Than Hsp104

(A) Luciferase aggregates were treated with the indicated combination of *E. coli* WT cytosol, *E. coli* Δ*clpb* cytosol, ClpB, yeast WT cytosol, yeast Δ*hsp104* cytosol, or Hsp104. Luciferase reactivation was assessed (% of total recoverable activity). Values represent means ±SEM (n = 3).

(B–D) Disordered luciferase aggregates (B), disordered GFP aggregates (C), or disordered CS aggregates (D) were treated with ClpB, DnaK, DnaJ, and GrpE or Hsp104, Ssa1, and Sis1. Reactivation was then assessed (% of total recoverable activity). Values represent means ±SEM (n = 3).

See also Table S1.

ClpB Reactivates Disordered Aggregates More Effectively Than Hsp104

E. coli cytosol was more active than yeast cytosol in reactivating aggregated luciferase, whereas Δ*clpb E. coli* cytosol was inactive but could be rescued by pure ClpB (Figure 3A). Accordingly, ClpB was more effective than Hsp104 in disordered aggregate dissolution (Figures 3B–3D). Thus, ClpB appears more adapted to resolve disordered aggregates that accrue upon protein-folding stress but is ineffective against amyloid.

Hsp104 Uses a Distinct Mechanism to Resolve Toxic Oligomers and Amyloids

Next, we analyzed Hsp104-catalyzed disassembly of toxic preamyloid oligomers and amyloid formed by the PD-linked α-syn^{A30P} and Ure2 prions. Disassembly of α-syn^{A30P} oligomers, α-syn^{A30P} amyloid, and Ure2 prions by Hsp104 was very sensitive to Hsp104^{DPL} (Figures 4A–4C), Hsp104^{DWA} (Figures 4D–4F), and Hsp104^{DPLDWB} (Figures 4G–4I). Hsp104's ability to disassemble α-Syn^{A30P} oligomers was abolished by approximately two mutant subunits per hexamer (Figures 4A, 4D, and 4G), whereas α-Syn^{A30P} amyloid and Ure2 prion disassembly were ablated by one mutant subunit per hexamer (Figures 4B, 4C, 4E, 4F, 4H, and 4I). Thus, more subunits must work together to disaggregate amyloid compared to disordered aggregates. These data suggest that Hsp104 hexamers switch to a highly cooperative mode of ATP hydrolysis and substrate handling to disassemble preamyloid oligomers and amyloids.

The response to mutant subunits (Hsp104^{DPL}, Hsp104^{DWA}, and Hsp104^{DPLDWB}) was invariant for amyloid remodeling, whereas the same mutant subunits elicit diverse responses in disordered aggregate dissolution (e.g., compare Figures 4B, 4E, and 4H to Figures 1F, 1G, and 1I). Thus, amyloids make more stringent demands on how Hsp104 subunits must collaborate to promote disaggregation.

Missing cofactors might enable Hsp104 to disaggregate amyloid by using a probabilistic mechanism as for disordered

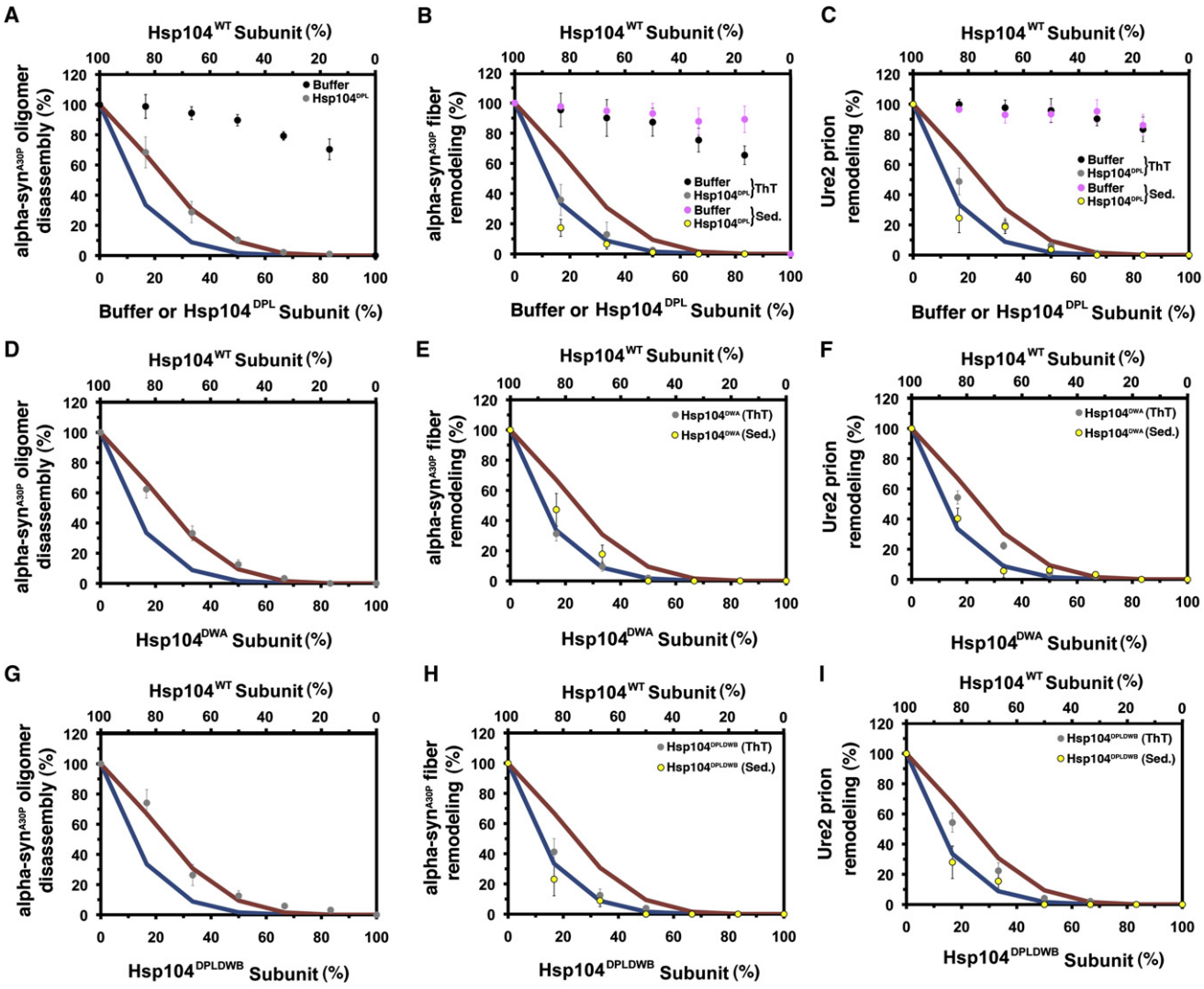

Figure 4. Hsp104 Exploits Cooperative Mechanisms to Remodel Preamyloid α-syn^{A30P} Oligomers, α-syn^{A30P} Amyloids, and Ure2 Prions

(A–I) α-syn^{A30P} oligomers (A, D, and G), α-syn^{A30P} amyloid (B, E, and H), or Ure2 prions (C, F, and I) were treated with Hsp104, Ssa1, and Sis1 plus increasing fractions of buffer (A, B, and C), Hsp104^{DPL} (A, B, and C), Hsp104^{DWA} (D, E, and F), or Hsp104^{DPLDWB} (G, H, and I). Oligomer remodeling was assessed by filter trap, and amyloid remodeling was assessed by ThT fluorescence (gray or black markers) or sedimentation (purple or yellow markers). Activity was converted to % WT activity. Values represent means ±SEM (n = 2–4). Expected activity if one or more (blue line [A–I]) or two or more (red line [A–I]) mutant subunits ablate hexamer activity.

See also Figure S4.

aggregates. For example, Hsp26 can assist Hsp104 in protein disaggregation (Duennwald et al., 2012). However, neither Hsp26 nor Δ*hsp104* yeast cytosol (to provide the entire cohort of molecular chaperones) altered the response of Hsp104 to Hsp104^{DPL} subunits in luciferase or Ure2 prion disaggregation (Figures S4C and S4D). Thus, missing cofactors are unlikely to alter the mechanism by which Hsp104 subunits collaborate to disaggregate disordered aggregates versus amyloid.

Hsp104 Switches Mechanism to Disaggregate Distinct Sup35 Prion Strains

Amyloidogenic proteins form structurally distinct amyloid "strains," which can vary in stability and confer distinct phenotypes (Cushman et al., 2010). Hsp104 subunits might collaborate differently to disaggregate distinct amyloid strains formed by the same protein. To examine this possibility, we exploited Sup35's prion domain, termed NM, which spontaneously forms different prion strains at different temperatures. NM prions formed at 4°C, termed NM4, possess a shorter, less stable amyloid core (T_m ~54°C) with distinctive intermolecular contacts and give rise to "strong" [*PSI*$^+$] variants in vivo (Krishnan and Lindquist, 2005) (Figure S5). Here, strength refers to the nonsense suppression phenotype caused by prion-mediated depletion of soluble Sup35 (Shorter and Lindquist, 2005). NM prions formed at 25 or 37°C, termed NM25 and NM37, harbor longer, more stable amyloid cores (T_m ~81°C for

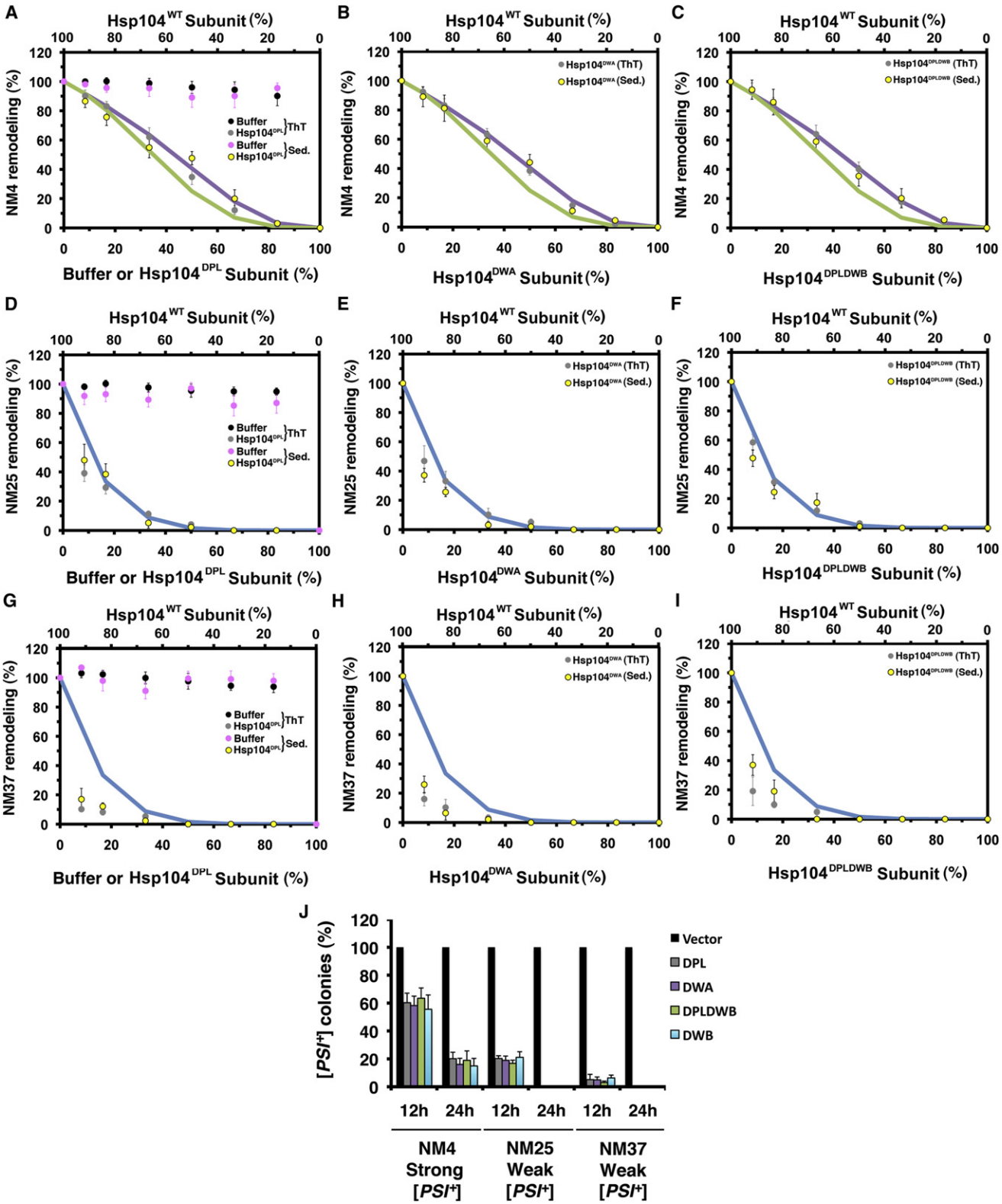

Figure 5. Hsp104 Switches Mechanism to Remodel Distinct Sup35 Prion Strains

(A–I) NM4, NM25, or NM37 prions were treated with Hsp104, Ssa1, and Sis1 plus increasing fractions of buffer (A, D, and G), $Hsp104^{DPL}$ (A, D, and G), $Hsp104^{DWA}$ (B, E, and H), or $Hsp104^{DPLDWB}$ (C, F, and I). Remodeling was monitored by ThT fluorescence (gray or black markers) or sedimentation (purple or yellow markers).

NM25 and T_m ~86°C for NM37) with intermolecular contacts distinct from NM4 and give rise to "weak" [*PSI*$^+$] variants in vivo (Krishnan and Lindquist, 2005) (Figure S5). NM4, NM25, and NM37 provide an opportunity to assess Hsp104 activity against alternative prion structures formed by the same primary sequence.

Remodeling each NM prion strain required a different mode of intersubunit collaboration by Hsp104. Thus, NM4 remodeling was less sensitive than NM25 or NM37 to Hsp104^{DPL} (Figures 5A, 5D, and 5G), Hsp104^{DWA} (Figures 5B, 5E, and 5H), Hsp104^{DPLDWB} (Figures 5C, 5F, and 5I), or Hsp104^{DWB} (data not shown). NM4 remodeling was ablated by approximately three to four mutant subunits per hexamer, whereas NM25 remodeling was ablated by one mutant subunit per hexamer (see Figure 1B). NM37 remodeling was unusually sensitive to mutant subunits (Figures 5G–5I), suggesting that more than one hexamer is needed to remodel this strain. Thus, as the length of the cross-β core of the NM prion increases and encroaches further into C-terminal sequence (Figure S5), the mechanism by which Hsp104 subunits collaborate switches to become more cooperative. For NM4, a subglobal cooperative mechanism will suffice, whereas NM25 requires global cooperativity.

Next, we tested the efficacy by which mutant Hsp104 subunits disrupt propagation of different [*PSI*$^+$] variants by Hsp104 in vivo (Chernoff et al., 1995). In accord with our in vitro data, Hsp104^{DPL}, Hsp104^{DWA}, Hsp104^{DWB}, and Hsp104^{DPLDWB} more readily disrupted propagation of weak [*PSI*$^+$] encoded by NM37 or NM25 than propagation of strong [*PSI*$^+$] encoded by NM4 (Figure 5J). Thus, Hsp104-driven remodeling of weak [*PSI*$^+$] prions (NM25 and NM37) is more sensitive to Hsp104^{DPL}, Hsp104^{DWA}, Hsp104^{DWB}, and Hsp104^{DPLDWB} subunits than Hsp104-driven remodeling of strong [*PSI*$^+$] prions (NM4) in vitro and in vivo (Figures 5A–5J). Importantly, these Hsp104 variants were equally effective in disrupting the Hsp104-catalyzed remodeling of a given [*PSI*$^+$] variant in vitro and in vivo (Figures 5A–5J). Unlike their effects on thermotolerance or in vivo luciferase reactivation, Hsp104^{DWB} was not a more effective dominant negative than Hsp104^{DPL} or Hsp104^{DPLDWB} (Figures 1J–1L and 5J). Thus, the mechanism by which Hsp104 remodels prions versus disordered aggregates differs in vivo.

Hsp104 Switches Mechanism to Disaggregate Disordered Aggregates versus Prions

We confirmed that Hsp104 switches mechanism to resolve disordered aggregates versus prions by using two strategies that do not employ mutant subunits. First, we used p370, a short peptide that competitively inhibits Hsp104-substrate binding (Lum et al., 2008). Importantly, Hsp104-catalyzed luciferase reactivation was insensitive to a 20-fold excess of p370, whereas NM4 remodeling was inhibited and NM37 remodeling was abolished (Figure 6A). A negative control peptide, pSGG, had no effect (Figure 6A). Thus, in accord with Hsp104^{DPL} doping (Figures 1F, 5B, and 5H), amyloid disaggregation by Hsp104 is more sensitive to inhibition of substrate binding than disordered aggregate dissolution.

Next, we examined the effect of various ratios of ATP and ATPγS, a slowly hydrolyzable ATP analog. We kept the total nucleotide concentration constant but varied the ATP:ATPγS ratio from 12:0 to 0:12. Luciferase reactivation by Hsp104, Hsp70, and Hsp40 was largely unaffected by increasing fractions of ATPγS. Optimal activity was observed at 7:5 or 6:6 ATP:ATPγS, and a ratio of 4:8 ATP:ATPγS supported activity similar to reactions with just ATP (Figure 6B). Activity was even detected at 1:11 ATP:ATPγS (Figure 6B). Hsp104 alone was inactive with ATP, but addition of ATPγS unleashed activity, and a 6:6 ATP:ATPγS ratio elicited maximal Hsp104 activity (Figure 6B). These activity profiles illustrate the adaptability of the Hsp104 hexamer, which can effectively disaggregate luciferase when diverse ATP:ATPγS mixtures populate its NBDs. In contrast, Hsp104-catalyzed remodeling of NM4 was sharply inhibited by low fractions of ATPγS, and NM37 was even more sensitive (Figures 6C and 6D). Thus, WT Hsp104 uses a distinct mechanism to disaggregate disordered aggregates versus amyloid.

Key Middle Domain and NBD2 Residues Enable Hsp104 to Switch Mechanism

We hypothesized that Hsp104 variants that are functional in thermotolerance but defective in prion propagation in vivo might be unable to switch mechanism. We focused on Hsp104^{D704N} and Hsp104^{L462R}, which confer WT thermotolerance but cannot propagate [*PSI*$^+$], [*RNQ*$^+$], or [*URE3*] (Kurahashi and Nakamura, 2007). D704 is between the NBD2 Walker B and sensor-1 motifs, whereas L462 is in helix 2 of the middle domain. D704 is predicted to contact the middle domain, whereas L462 is predicted to be in proximity to nucleotide in NBD1 (Wendler et al., 2007). Thus, D704 and L462 could mediate the interdomain or intersubunit communication necessary to switch mechanism.

In vitro, Hsp104^{D704N} had reduced ATPase activity, whereas Hsp104^{L462R} had WT levels of ATPase activity (Figure 6E). Both mutants had reduced ability to reactivate luciferase aggregates and could not remodel NM25 (Figure 6E), which explains their ability to confer thermotolerance, but not prion propagation, in vivo (Kurahashi and Nakamura, 2007). Very little functional Hsp104 is required for thermotolerance (Lindquist and Kim, 1996). Thus, reduced Hsp104^{D704N} or Hsp104^{L462R} activity against disordered aggregates is likely sufficient for thermotolerance, especially when cells are given a conditioning pretreatment.

The limited ability of Hsp104^{D704N} and Hsp104^{L462R} to remodel amyloid is reminiscent of ClpB (Figures 2C and 2D). Thus, Hsp104^{D704N} and Hsp104^{L462R} subunits might also collaborate differently than WT Hsp104 subunits to dissolve disordered aggregates. To probe how Hsp104^{D704N} and Hsp104^{L462R} subunits collaborate in luciferase reactivation, we doped in mutant Hsp104^{D704N} and Hsp104^{L462R} subunits defective in

Activity was converted to % WT activity. Values represent means ±SEM (n = 2–4). Expected activity if four or more (purple line [A–C]), three or more (green line [A–C]), or one or more (blue line [D–I]) mutant subunits ablate hexamer activity.
(J) Strong and weak [*PSI*$^+$] curing by Hsp104^{DPL}, Hsp104^{DWA}, Hsp104^{DPLDWB}, or Hsp104^{DWB} overexpression. Values represent means ±SEM (n = 3).
See also Figure S5.

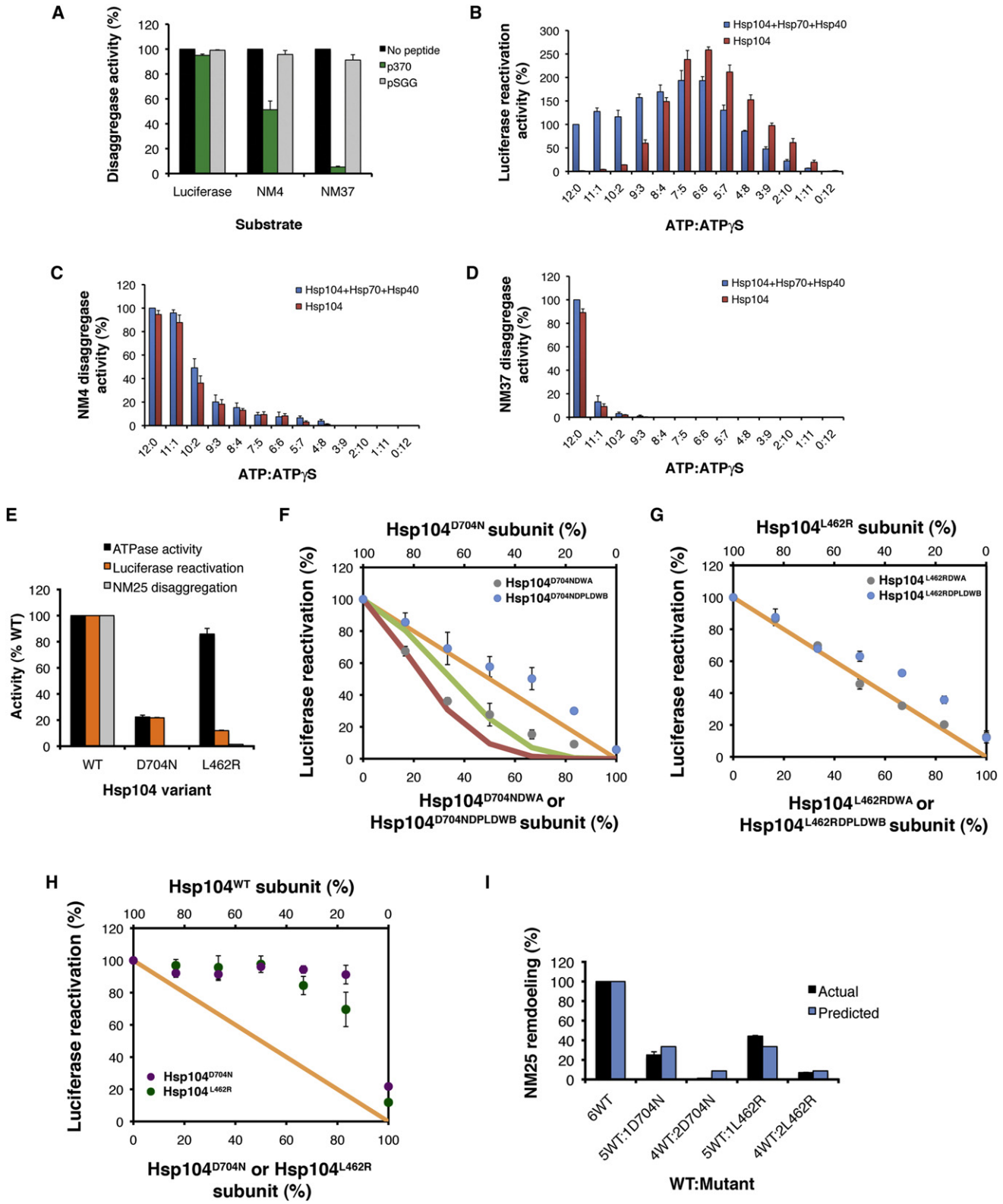

Figure 6. Selective Ablation of Amyloid Disaggregase Activity by p370, ATPγS, Hsp104^{D704N}, or Hsp104^{L462R} Subunits

(A) Luciferase aggregates, NM4 prions, or NM37 prions were treated with Hsp104, Ssa1, and Sis1 plus buffer, p370, or pSGG. Disaggregase activity was converted to % activity in the absence of peptide. Values represent means ±SEM (n = 2).

ATP hydrolysis (DWA) or ATP hydrolysis and substrate binding (DPLDWB). For Hsp104^{D704N}, activity declined sharply upon doping Hsp104^{D704NDWA}, which is consistent with two to three mutant subunits inactivating the Hsp104^{D704N} hexamer (Figure 6F). Thus, Hsp104^{D704N} exploits a subglobally cooperative mechanism of ATP hydrolysis to reactivate luciferase, unlike WT Hsp104, which uses a probabilistic mechanism (Figure 1G). Indeed, Hsp104^{D704N} responds to ATPase-defective subunits more like ClpB (Figure 1G), which has limited amyloid-remodeling activity (Figures 2C and 2D). Hsp104^{D704NDPLDWB} subunits elicited an approximately linear decline in Hsp104^{D704N} luciferase reactivation activity (Figure 6F) rather than the stimulation observed with WT Hsp104 or sharp inhibition observed with ClpB (Figure 1I). Unlike WT Hsp104, Hsp104^{D704N} subunits with defective ATPase and substrate-binding activity do not stimulate adjacent Hsp104^{D704N} subunits. Thus, D704N impairs intersubunit communication and precludes amyloid disaggregation.

Hsp104^{L462R} subunits collaborated differently than Hsp104^{D704N} and WT Hsp104 subunits to disaggregate luciferase. Doping Hsp104^{L462RDWA} caused a roughly linear decline in Hsp104^{L462R} activity, indicating a probabilistic mechanism akin to WT Hsp104 (Figures 1G and 6G). Doping Hsp104^{L462RDPLDWB} elicited a roughly linear decline in Hsp104^{L462R} luciferase reactivation activity rather than the stimulation observed with WT Hsp104 (Figures 1I and 6G). Thus, Hsp104^{L462R} subunits with defective ATPase and substrate-binding activity do not stimulate adjacent Hsp104^{L462R} subunits. We conclude that L462R disrupts intersubunit communication and ablates amyloid remodeling.

Doping Hsp104^{D704N} or Hsp104^{L462R} subunits had little effect on luciferase reactivation by WT Hsp104, even though Hsp104^{D704N} and Hsp104^{L462R} are ~5–9-fold less active than WT Hsp104 against luciferase (Figures 6E and 6H). These data reillustrate the resilience of the Hsp104 hexamer and its capacity to accommodate defective subunits and still effectively resolve disordered aggregates. Even an average of one WT subunit per Hsp104^{D704N} or Hsp104^{L462R} hexamer is capable of catalyzing the same amount of disaggregation as a WT hexamer (Figure 6H). By contrast, Hsp104^{D704N} or Hsp104^{L462R} subunits caused a sharp decline in Hsp104-catalyzed NM25 remodeling consistent with one mutant subunit disrupting hexamer activity (Figure 6I). Thus, D704 and L462 likely transmit or receive signals that recruit additional Hsp104 subunits for amyloid disaggregation. Impairing intersubunit communication with specific mutations, such as D704N or L462R, yields Hsp104 variants that dissolve disordered aggregates, but not amyloid.

DISCUSSION

We have established that Hsp104 employs distinct modes of intersubunit collaboration to resolve disordered aggregates versus amyloid. For disordered aggregates, Hsp104 subunits use probabilistic ATP hydrolysis similar to the mechanism defined for ClpX, a protein unfoldase (Martin et al., 2005). However, unlike ClpX, Hsp104 withstands subunits that cannot bind substrate. ClpX hexamers are severely impaired by two subunits that cannot engage substrate (Martin et al., 2008), whereas Hsp104 retains ~70% activity. This sensitivity might explain why ClpX is a poor protein disaggregase (Doyle et al., 2007a).

The permissive nature of Hsp104 hexamers to subunits that cannot hydrolyze ATP or engage substrate enables a highly flexible disaggregase. Thus, one WT subunit per hexamer is sufficient to catalyze disaggregation (Figure 7A). Indeed, any opportunely positioned subunit within the hexamer that can hydrolyze ATP and engage the irregular and heterogeneous aggregated structure can promote disaggregation. Individual subunits do not have to coordinate ATPase or substrate-binding events with neighboring subunits or wait until all subunits are engaged, which may be sterically improbable. Thus, Hsp104 can resolve the unrelated proteins of the aggregated proteome after stress.

Surprisingly, ClpB, the *E. coli* homolog of Hsp104, is tuned differently to Hsp104. Like Hsp104, ClpB exploits probabilistic substrate binding to dissolve disordered aggregates and tolerates subunits that cannot bind substrate (Figure 7B). This shared feature of ClpB and Hsp104 distinguishes them from the protein unfoldase, ClpX.

Unlike Hsp104, ClpB couples probabilistic substrate binding to highly cooperative ATP hydrolysis (Figure 7B). Unexpectedly, this operating mode enables ClpB to dissolve disordered aggregates more effectively than Hsp104. However, this enhancement comes at the expense of robust disaggregase

(B) Luciferase aggregates were treated with Hsp104, Hsc70, and Hdj2 or Hsp104 alone plus various ATP:ATPγS ratios. Disaggregase activity was converted to % activity of Hsp104, Hsc70, and Hdj2 plus ATP. Values represent means ±SEM (n = 3).

(C and D) NM4 prions (C) or NM37 prions (D) were treated with Hsp104, Ssa1, and Sis1 or Hsp104 alone plus various ATP:ATPγS ratios. Disaggregase activity was converted to % activity of Hsp104, Ssa1, and Sis1 plus ATP. Values represent means ±SEM (n = 3).

(E) Comparison of ATPase activity, luciferase reactivation activity, and NM25 disaggregase activity of WT Hsp104, Hsp104^{D704N}, and Hsp104^{L462R}. Observed activity was converted to % WT activity. Values represent means ±SEM (n = 2–3).

(F) Luciferase aggregates were treated with Hsp104^{D704N}, Hsc70, and Hdj2 plus increasing fractions of Hsp104^{D704NDWA} (gray markers) or Hsp104^{D704NDPLDWB} (blue markers). Luciferase reactivation was converted to % Hsp104^{D704N} activity. Expected activity if six (orange line), three or more (green line), or two or more (red line) mutant subunits ablate hexamer activity. Values represent means ±SEM (n = 3).

(G) Luciferase aggregates were treated with Hsp104^{L462R}, Hsc70, and Hdj2 plus increasing fractions of Hsp104^{L462RDWA} (gray markers) or Hsp104^{L462RDPLDWB} (blue markers). Luciferase reactivation was converted to % Hsp104^{L462R} activity. Orange line indicates expected activity if six mutant subunits are needed to ablate hexamer activity. Values represent means ±SEM (n = 3).

(H) Luciferase aggregates were treated with Hsp104, Hsc70, and Hdj2 plus increasing fractions of Hsp104^{D704N} (purple markers) or Hsp104^{L462R} (green markers). Luciferase reactivation was converted to % WT Hsp104 activity. Orange line indicates expected activity if six mutant subunits are needed to ablate hexamer activity. Values represent means ±SEM (n = 2).

(I) NM25 was treated with Hsp104, Ssa1, and Sis1 plus increasing fractions of Hsp104^{D704N} or Hsp104^{L462R}. Remodeling was monitored by ThT fluorescence. Activity was converted to % WT Hsp104 activity. Predicted activity (blue bars) if one mutant subunit ablates hexamer activity. Values represent means ±SEM (n = 2).

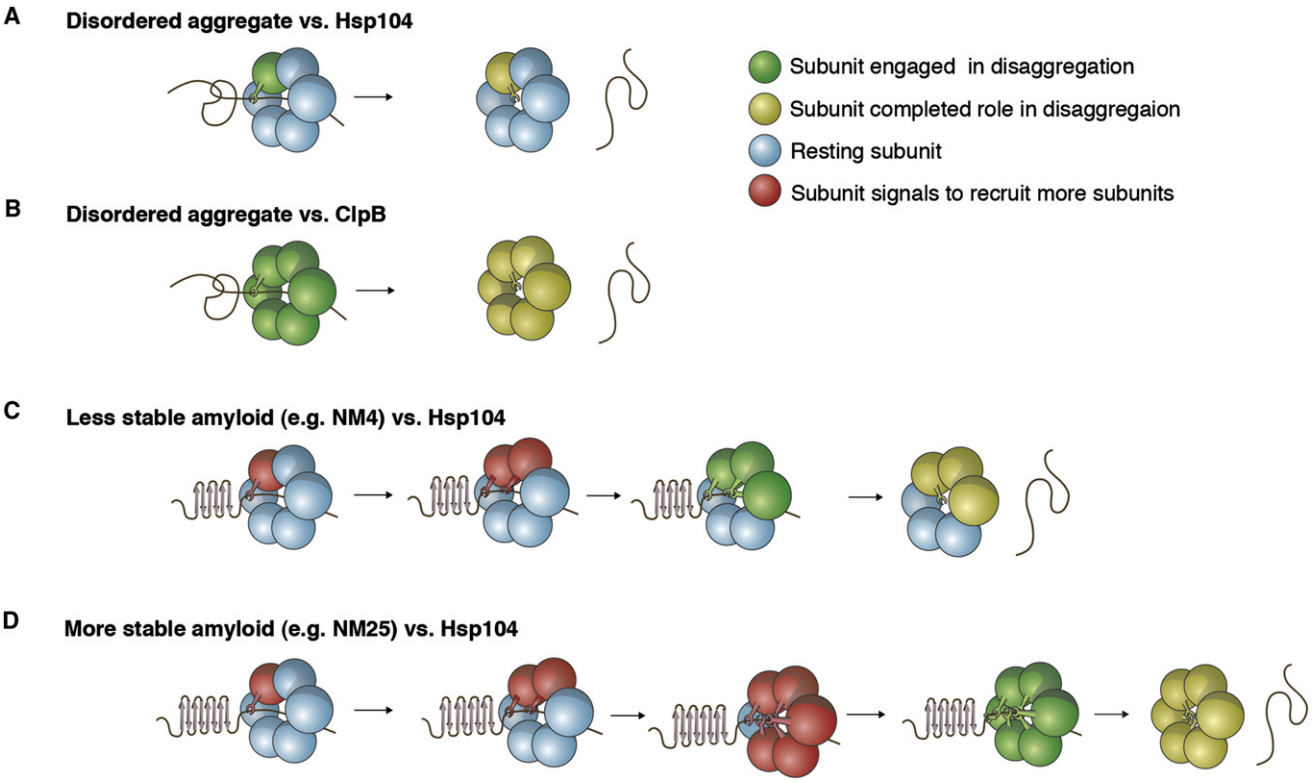

Figure 7. Mechanisms of Intersubunit Collaboration for Hsp104 and ClpB

(A–D) Hsp104 (A, C, and D) or ClpB (B) subunits are depicted as spheres, and a single aggregated conformer is displayed. Green subunits are engaged in productive disaggregation via substrate binding (depicted by a lever) and/or ATP hydrolysis. Yellow subunits have completed their role in disaggregation. Blue subunits are resting and do not need to hydrolyze ATP or engage substrate for successful disaggregation. Red subunits recruit resting subunits until a sufficient number are recruited to promote disaggregation.

(A) Hsp104 couples probabilistic ATPase activity and substrate binding to resolve disordered aggregates. Thus, a single subunit within a hexamer that can bind substrate and hydrolyze ATP is sufficient to drive protein disaggregation.

(B) ClpB exploits cooperative ATPase activity and probabilistic substrate binding to resolve disordered aggregates. Five or six ClpB subunits per hexamer must hydrolyze ATP to disaggregate disordered aggregates. Cooperative ATPase activity is not coupled to cooperative substrate handling, as one ClpB subunit capable of binding substrate can drive disaggregation provided five or six subunits can hydrolyze ATP.

(C) Hsp104 switches to a subglobal cooperative mechanism of ATP hydrolysis and substrate binding to resolve NM4 prions. One subunit initially engages amyloid, but the localized structural stability of the cross-β form antagonizes unfolding, which elicits a signal (red subunit) that recruits additional subunits until a sufficient number are recruited that can together unfold the cross-β structure. For NM4, three subunits per hexamer must engage substrate and hydrolyze ATP.

(D) Hsp104 switches to a global cooperative mechanism of ATP hydrolysis and substrate binding to resolve more refractory amyloids, such as NM25 prions. Hsp104 subunits collaborate as in (C) except that the local stability of the amyloid fold is even more antagonistic, such that six subunits must be recruited to engage substrate and hydrolyze ATP for disaggregation.

activity able to accommodate ATPase-defective subunits. Unlike Hsp104, ClpB hexamers cannot tolerate a single ATPase-defective subunit. Our data also suggest that, unlike Hsp104, ClpB has limited ability to couple cooperative ATPase activity to cooperative substrate handling, which is necessary to remodel amyloid.

The robustness and plasticity of Hsp104 hexamers are likely an adaptation that enables amyloid remodeling and empowers yeast to exploit prions for beneficial purposes. Indeed, ClpB and *E. coli* cytosol were unable to remodel amyloid. Amyloid can accumulate in *E. coli* upon protein overexpression (Wang et al., 2008). Yet, ClpB's limited amyloid-remodeling activity suggests that *E. coli* compartmentalizes amyloid rather than disseminating it throughout the cytoplasm. Yeast also partition amyloid, but simultaneously disperse cytosolic prions for beneficial purposes. The profound selective advantages afforded by yeast prions are only made possible by Hsp104's potent amyloid-remodeling activity (Alberti et al., 2009; Halfmann et al., 2012; Shorter and Lindquist, 2005).

We suggest that Hsp104's default intersubunit collaboration mechanism is probabilistic (Figure 7A). However, this default-operating mode can be rapidly retuned to a suitable subglobal or global cooperative mechanism upon sensing stable substrates. Thus, amyloid likely antagonizes unfolding and elicits a signal for Hsp104 subunits to work together to engage substrate, hydrolyze ATP, and promote disaggregation (Figures 7C and 7D). For less chemically stable NM4 prions, a subglobal cooperative mechanism that is inactivated by three mutant subunits per hexamer is employed (Figure 7C). By contrast, NM25 prions, which

are more stable and possess a longer cross-β core, are resolved by a global cooperative mechanism that is inactivated by one mutant subunit (Figure 7D). Ure2 prions and α-syn^{A30P} amyloid are also resolved in this way (Figure 7D). Cryo-EM reconstructions indicate that Hsp104 might use a cooperative, sequential mechanism of substrate handling (Wendler et al., 2009). However, we suggest that hexamer plasticity enables Hsp104 to adapt a variety of mechanochemical coupling mechanisms that are responsive to the specific physical demands of the aggregated substrate. Thus, Hsp104 is wired do the minimum work necessary to disaggregate any given substrate, i.e., if two subunits are sufficient to rapidly disaggregate a substrate, then only two will be used. Various multimeric, NTP-fueled ring-translocases with diverse substrate portfolios could use similar adaptable repertoires of intersubunit collaboration.

We establish that D704N or L462R mutations impair intersubunit communication, reduce plasticity, and selectively ablate amyloid disaggregation. Indeed, D704 and L462 likely transmit or receive signals to recruit additional Hsp104 subunits during prion disaggregation (Figures 7C and 7D). Although further studies are needed to gain a structural understanding of how Hsp104 switches mechanism, our findings explain why Hsp104^{D704N} and Hsp104^{L462R} are functional in thermotolerance but are defective in prion propagation (Kurahashi and Nakamura, 2007).

Hsp104 might be designed to be more potent and selective against specific proteins, which could empower facile purification of irksome recombinant proteins for basic or therapeutic purposes. Hsp104 could also be developed to target select misfolded proteins in neurodegenerative disease (Vashist et al., 2010). The intrinsic ability of Hsp104 to remodel diverse disease-associated amyloids as well as toxic oligomers suggests that this avenue warrants exploration. Here, it will be key to increase the specificity of the Hsp104 hexamer for a target polypeptide while simultaneously tuning plasticity such that toxic conformers are selectively eradicated. For example, hypomorphic scaffolds based on Hsp104^{D704N} or Hsp104^{L462R} could be useful in settings in which amyloids are protective and disordered aggregates are toxic.

EXPERIMENTAL PROCEDURES

Modeling Heterohexamer Ensemble Activity

The bionomial distribution was used to simulate the activity of various heterohexamer ensembles (Werbeck et al., 2008):

$$p(x) = \binom{n}{x} p^x (1-p)^{n-x}$$

where P is the probability that a hexamer (therefore, n = 6) contains x mutant subunits, and p is the probability that a mutant subunit is incorporated. Subunit mixing experiments demonstrated that mutant and WT subunits have a similar probability of being incorporated into a hexamer (Figures S1D–S1I and S2J; see Extended Experimental Procedures). Consequently, p is calculated as the molar ratio of mutant and WT protein present:

$$p = \frac{Hsp104_{mut}}{(Hsp104_{mut} + Hsp104_{WT})}$$

Therefore, for any specified percentage of mutant subunits, the probability distribution of Hsp104 hexamers containing zero, one, two, three, four, five, or six mutant subunits can be derived (Figure 1A). Activity versus p plots (Figure 1B) could then be generated assuming each WT subunit makes an equal contribution to the total activity (one-sixth per subunit). For more details, see Extended Experimental Procedures.

Proteins

Proteins were purified by using standard protocols as described (Shorter and Lindquist, 2004, 2006; Lo Bianco et al., 2008). For more details, see Extended Experimental Procedures.

Cytosol Preparation

Yeast and bacterial cytosol were prepared as described except that cells were lysed by using a French pressure cell (Glover and Lindquist, 1998) with modifications as detailed in Extended Experimental Procedures.

ATPase Assay

Hsp104 (0.25 μM monomer) comprising the indicated fraction of WT Hsp104 and mutant was equilibrated in luciferase refolding buffer (LRB; 25 mM HEPES-KOH [pH 7.4], 150 mM KAOc, 10 mM MgAOc, 10 mM DTT) for 15 min on ice and then incubated for 10 min at 25°C in the presence of ATP (1 mM). ATPase activity was assessed by the release of inorganic phosphate, which was determined by using a malachite green phosphate detection kit (Innova). For more details, see Extended Experimental Procedures.

Disaggregation Assays

Disaggregation of luciferase (50 nM), GFP (0.45 μM), CS (0.1 μM), various amyloids (1–2.5 μM), and α-syn^{A30P} oligomers (1 μM) was performed in the presence of Hsp104 or ClpB (0.167–20 μM) and the indicated Hsp70 (0.167–6 μM) and Hsp40 (0.033–6 μM) plus ATP and ATP regeneration system as described (Doyle et al., 2007b; Glover and Lindquist, 1998; Lo Bianco et al., 2008; Shorter and Lindquist, 2004, 2006). For reactions containing ClpB, GrpE (0.0167 μM) was also added. Total Hsp104 (or ClpB) was comprised of either WT or mutant subunit or a 1:5, 2:4, 3:3, 4:2, and 5:1 mixture of the two as indicated. WT and mutant mixtures were allowed to equilibrate for 15 min on ice prior to addition to the reaction. For more details, see Extended Experimental Procedures.

Thermotolerance, In Vivo Luciferase Reactivation, and [*PSI*$^+$] Curing Assays

In vivo thermotolerance, luciferase reactivation, and [*PSI*$^+$] curing assays were performed by using standard assays as described (Chernoff et al., 1995; Parsell et al., 1994: Wendler et al., 2007). Briefly, for thermotolerance, cells were transferred to 50°C for 0–20 min and then spotted or plated on SGal-ura media and grown at 30°C to monitor survival. For luciferase reactivation, cells were shifted to 44°C for 60 min and then allowed to recover in the presence of cycloheximide (10 μg/ml) at 30°C for 90 min, at which time luciferase activity was determined. For [*PSI*$^+$] curing, cells carrying the indicated plasmids were maintained in midlog growth phase by dilution with SRafGal-ura media and plated on 25% YPD. [*PSI*$^+$] curing was then scored as the proportion of red ade$^-$ [*psi*$^-$] colonies. For more details, see Extended Experimental Procedures.

SUPPLEMENTAL INFORMATION

Supplemental Information includes Extended Experimental Procedures, five figures, and one table and can be found with this article online at http://dx.doi.org/10.1016/j.cell.2012.09.038.

ACKNOWLEDGMENTS

We thank Sue Lindquist, Sabine Kedzierska-Mieszkowska, and Virginia Lee for reagents. We thank Sandra Maday, Mark Lemmon, Aaron Gitler, Walter Englander, and Nancy Bonini for critiques and Lili Guo for artwork. Our work was funded by NIH training grant T32GM071339 and NRSA predoctoral fellowship F31NS079009 (M.E.D.); NIH training grant T32GM008275 (E.A.S. and M.A.S.); AHA predoctoral (E.A.S.) and postdoctoral fellowships (M.E.J.); NIH training grant T32AG000255 and NRSA predoctoral fellowship F31NS067890 (M.C.-N.); NIH Director's New Innovator Award (DP2OD002177), Ellison Medical

Foundation New Scholar in Aging Award, Penn Institute of Aging, Alzheimer Disease Core Center, and Diabetes Research Center Awards (J.S.).

Received: September 16, 2011
Revised: June 25, 2012
Accepted: September 20, 2012
Published: November 8, 2012

REFERENCES

Alberti, S., Halfmann, R., King, O., Kapila, A., and Lindquist, S. (2009). A systematic survey identifies prions and illuminates sequence features of prionogenic proteins. Cell *137*, 146–158.

Barnhart, M.M., and Chapman, M.R. (2006). Curli biogenesis and function. Annu. Rev. Microbiol. *60*, 131–147.

Bösl, B., Grimminger, V., and Walter, S. (2005). Substrate binding to the molecular chaperone Hsp104 and its regulation by nucleotides. J. Biol. Chem. *280*, 38170–38176.

Chernoff, Y.O., Lindquist, S.L., Ono, B., Inge-Vechtomov, S.G., and Liebman, S.W. (1995). Role of the chaperone protein Hsp104 in propagation of the yeast prion-like factor [*PSI*$^{+}$]. Science *268*, 880–884.

Cohen, E., Bieschke, J., Perciavalle, R.M., Kelly, J.W., and Dillin, A. (2006). Opposing activities protect against age-onset proteotoxicity. Science *313*, 1604–1610.

Cushman, M., Johnson, B.S., King, O.D., Gitler, A.D., and Shorter, J. (2010). Prion-like disorders: blurring the divide between transmissibility and infectivity. J. Cell Sci. *123*, 1191–1201.

Dandoy-Dron, F., Bogdanova, A., Beringue, V., Bailly, Y., Tovey, M.G., Laude, H., and Dron, M. (2006). Infection by ME7 prion is not modified in transgenic mice expressing the yeast chaperone Hsp104 in neurons. Neurosci. Lett. *405*, 181–185.

Doyle, S.M., and Wickner, S. (2009). Hsp104 and ClpB: protein disaggregating machines. Trends Biochem. Sci. *34*, 40–48.

Doyle, S.M., Hoskins, J.R., and Wickner, S. (2007a). Collaboration between the ClpB AAA+ remodeling protein and the DnaK chaperone system. Proc. Natl. Acad. Sci. USA *104*, 11138–11144.

Doyle, S.M., Shorter, J., Zolkiewski, M., Hoskins, J.R., Lindquist, S., and Wickner, S. (2007b). Asymmetric deceleration of ClpB or Hsp104 ATPase activity unleashes protein-remodeling activity. Nat. Struct. Mol. Biol. *14*, 114–122.

Duennwald, M.L., Echeverria, A., and Shorter, J. (2012). Small heat shock proteins potentiate amyloid dissolution by protein disaggregases from yeast and humans. PLoS Biol. *10*, e1001346.

Garrity, S.J., Sivanathan, V., Dong, J., Lindquist, S., and Hochschild, A. (2010). Conversion of a yeast prion protein to an infectious form in bacteria. Proc. Natl. Acad. Sci. USA *107*, 10596–10601.

Glover, J.R., and Lindquist, S. (1998). Hsp104, Hsp70, and Hsp40: a novel chaperone system that rescues previously aggregated proteins. Cell *94*, 73–82.

Halfmann, R., Jarosz, D.F., Jones, S.K., Chang, A., Lancaster, A.K., and Lindquist, S. (2012). Prions are a common mechanism for phenotypic inheritance in wild yeasts. Nature *482*, 363–368.

Hattendorf, D.A., and Lindquist, S.L. (2002). Cooperative kinetics of both Hsp104 ATPase domains and interdomain communication revealed by AAA sensor-1 mutants. EMBO J. *21*, 12–21.

Hoskins, J.R., Doyle, S.M., and Wickner, S. (2009). Coupling ATP utilization to protein remodeling by ClpB, a hexameric AAA+ protein. Proc. Natl. Acad. Sci. USA *106*, 22233–22238.

Knowles, T.P., Fitzpatrick, A.W., Meehan, S., Mott, H.R., Vendruscolo, M., Dobson, C.M., and Welland, M.E. (2007). Role of intermolecular forces in defining material properties of protein nanofibrils. Science *318*, 1900–1903.

Krishnan, R., and Lindquist, S.L. (2005). Structural insights into a yeast prion illuminate nucleation and strain diversity. Nature *435*, 765–772.

Kurahashi, H., and Nakamura, Y. (2007). Channel mutations in Hsp104 hexamer distinctively affect thermotolerance and prion-specific propagation. Mol. Microbiol. *63*, 1669–1683.

Lee, S., Sielaff, B., Lee, J., and Tsai, F.T. (2010). CryoEM structure of Hsp104 and its mechanistic implication for protein disaggregation. Proc. Natl. Acad. Sci. USA *107*, 8135–8140.

Lindquist, S., and Kim, G. (1996). Heat-shock protein 104 expression is sufficient for thermotolerance in yeast. Proc. Natl. Acad. Sci. USA *93*, 5301–5306.

Lo Bianco, C., Shorter, J., Régulier, E., Lashuel, H., Iwatsubo, T., Lindquist, S., and Aebischer, P. (2008). Hsp104 antagonizes alpha-synuclein aggregation and reduces dopaminergic degeneration in a rat model of Parkinson disease. J. Clin. Invest. *118*, 3087–3097.

Lum, R., Niggemann, M., and Glover, J.R. (2008). Peptide and protein binding in the axial channel of Hsp104. Insights into the mechanism of protein unfolding. J. Biol. Chem. *283*, 30139–30150.

Lyubimov, A.Y., Strycharska, M., and Berger, J.M. (2011). The nuts and bolts of ring-translocase structure and mechanism. Curr. Opin. Struct. Biol. *21*, 240–248.

Martin, A., Baker, T.A., and Sauer, R.T. (2005). Rebuilt AAA + motors reveal operating principles for ATP-fuelled machines. Nature *437*, 1115–1120.

Martin, A., Baker, T.A., and Sauer, R.T. (2008). Protein unfolding by a AAA+ protease is dependent on ATP-hydrolysis rates and substrate energy landscapes. Nat. Struct. Mol. Biol. *15*, 139–145.

Moreau, M.J., McGeoch, A.T., Lowe, A.R., Itzhaki, L.S., and Bell, S.D. (2007). ATPase site architecture and helicase mechanism of an archaeal MCM. Mol. Cell *28*, 304–314.

Parsell, D.A., Kowal, A.S., Singer, M.A., and Lindquist, S. (1994). Protein disaggregation mediated by heat-shock protein Hsp104. Nature *372*, 475–478.

Reidy, M., Miot, M., and Masison, D.C. (2012). Prokaryotic chaperones support yeast prions and thermotolerance and define disaggregation machinery interactions. Genetics *192*, 185–193.

Schirmer, E.C., Ware, D.M., Queitsch, C., Kowal, A.S., and Lindquist, S.L. (2001). Subunit interactions influence the biochemical and biological properties of Hsp104. Proc. Natl. Acad. Sci. USA *98*, 914–919.

Shorter, J. (2011). The mammalian disaggregase machinery: Hsp110 synergizes with Hsp70 and Hsp40 to catalyze protein disaggregation and reactivation in a cell-free system. PLoS ONE *6*, e26319.

Shorter, J., and Lindquist, S. (2004). Hsp104 catalyzes formation and elimination of self-replicating Sup35 prion conformers. Science *304*, 1793–1797.

Shorter, J., and Lindquist, S. (2005). Prions as adaptive conduits of memory and inheritance. Nat. Rev. Genet. *6*, 435–450.

Shorter, J., and Lindquist, S. (2006). Destruction or potentiation of different prions catalyzed by similar Hsp104 remodeling activities. Mol. Cell *23*, 425–438.

Tessarz, P., Mogk, A., and Bukau, B. (2008). Substrate threading through the central pore of the Hsp104 chaperone as a common mechanism for protein disaggregation and prion propagation. Mol. Microbiol. *68*, 87–97.

Vacher, C., Garcia-Oroz, L., and Rubinsztein, D.C. (2005). Overexpression of yeast hsp104 reduces polyglutamine aggregation and prolongs survival of a transgenic mouse model of Huntington's disease. Hum. Mol. Genet. *14*, 3425–3433.

Vashist, S., Cushman, M., and Shorter, J. (2010). Applying Hsp104 to protein-misfolding disorders. Biochem. Cell Biol. *88*, 1–13.

Wang, L., Maji, S.K., Sawaya, M.R., Eisenberg, D., and Riek, R. (2008). Bacterial inclusion bodies contain amyloid-like structure. PLoS Biol. *6*, e195.

Wang, L., Schubert, D., Sawaya, M.R., Eisenberg, D., and Riek, R. (2010). Multidimensional structure-activity relationship of a protein in its aggregated states. Angew. Chem. Int. Ed. Engl. *49*, 3904–3908.

Weibezahn, J., Schlieker, C., Bukau, B., and Mogk, A. (2003). Characterization of a trap mutant of the AAA+ chaperone ClpB. J. Biol. Chem. *278*, 32608–32617.

Weibezahn, J., Tessarz, P., Schlieker, C., Zahn, R., Maglica, Z., Lee, S., Zentgraf, H., Weber-Ban, E.U., Dougan, D.A., Tsai, F.T., et al. (2004). Thermotolerance requires refolding of aggregated proteins by substrate translocation through the central pore of ClpB. Cell *119*, 653–665.

Wendler, P., Shorter, J., Plisson, C., Cashikar, A.G., Lindquist, S., and Saibil, H.R. (2007). Atypical AAA+ subunit packing creates an expanded cavity for disaggregation by the protein-remodeling factor Hsp104. Cell *131*, 1366–1377.

Wendler, P., Shorter, J., Snead, D., Plisson, C., Clare, D.K., Lindquist, S., and Saibil, H.R. (2009). Motor mechanism for protein threading through Hsp104. Mol. Cell *34*, 81–92.

Werbeck, N.D., Schlee, S., and Reinstein, J. (2008). Coupling and dynamics of subunits in the hexameric AAA+ chaperone ClpB. J. Mol. Biol. *378*, 178–190.

Wickner, R.B., Edskes, H.K., Bateman, D., Kelly, A.C., and Gorkovskiy, A. (2011). The yeast prions [*PSI*$^{+}$] and [*URE*3] are molecular degenerative diseases. Prion *5*, 258–262.